Sea surface temperatures did not control the first occurrence of Hudson Strait Heinrich Events during MIS 16

B. David A. Naafs,[1,2] Jens Hefter,[1] Patrizia Ferretti,[3,4] Ruediger Stein,[1] and Gerald H. Haug[2,5]

[1] Hudson Strait (HS) Heinrich Events, ice-rafting events in the North Atlantic originating from the Laurentide ice sheet (LIS), are among the most dramatic examples of millennial-scale climate variability and have a large influence on global climate. However, it is debated as to whether the occurrence of HS Heinrich Events in the (eastern) North Atlantic in the geological record depends on greater ice discharge, or simply from the longer survival of icebergs in cold waters. Using sediments from Integrated Ocean Drilling Program (IODP) Site U1313 in the North Atlantic spanning the period between 960 and 320 ka, we show that sea surface temperatures (SSTs) did not control the first occurrence of HS Heinrich(-like) Events in the sedimentary record. Using mineralogy and organic geochemistry to determine the characteristics of ice-rafting debris (IRD), we detect the first HS Heinrich(-like) Event in our record around 643 ka (Marine Isotope Stage (MIS) 16), which is similar as previously reported for Site U1308. However, the accompanying high-resolution alkenone-based SST record demonstrates that the first HS Heinrich(-like) Event did not coincide with low SSTs. Thus, the HS Heinrich(-like) Events do indicate enhanced ice discharge from the LIS at the end of the Mid-Pleistocene Transition, not simply the survivability of icebergs due to cold conditions in the North Atlantic.

1. Introduction

[2] In the 1980s Heinrich discovered that sediments from the Dreizack Seamounts in the North Atlantic covering the last glacial cycle contained several layers that were rich in ice-rafted debris (IRD) [*Heinrich*, 1988]. These layers that now bear his name [*Broecker et al.*, 1992] have been found at many sites between ~40 and 55°N in the North Atlantic and have received much attention from the paleoclimate community over the past two decades [e.g., *Hemming*, 2004]. Besides the high flux of IRD, Heinrich layers have anomalously high magnetic susceptibility values and low abundance of foraminifera [e.g., *Broecker et al.*, 1992; *Grousset et al.*, 1993; *McManus et al.*, 1998]. Although six layers were originally identified for the last glacial cycle

(H1–6) [*Bond et al.*, 1992], it is debated whether H3 and 6 are truly ice-rafting events (at least in the eastern North Atlantic) and are not the result from low accumulation of foraminifera [*Gwiazda et al.*, 1996; *Hemming*, 2004]. The IRD of Heinrich layers 1, 2, 4, and 5 shares a set of characteristics that is consistent with an origin from Paleozoic carbonates in the Hudson area of Canada [*Hemming*, 2004]. This subgroup is termed Hudson Strait (HS) Heinrich Events and is related to instabilities of the Laurentide ice sheet (LIS) [*Hemming*, 2004; *Hodell et al.*, 2008]. As the LIS formed the largest ice sheet in the Northern Hemisphere during glacials it is reasonable to suggest that the HS Heinrich Events indicate the most intense periods of ice-rafting in the mid-latitude North Atlantic. This is also supported by the higher flux of IRD during these four events in the eastern North Atlantic [*McManus et al.*, 1998; *Hemming*, 2004].

[3] The massive input of icebergs from the LIS during (HS) Heinrich Events led to severe cooling and freshening of surface waters in one of the most sensitive regions of the world: the North Atlantic [*Bard et al.*, 2000; *Rosell-Melé et al.*, 2002]. Based on the most recent glacial cycle, a set of related hypotheses have arisen for a feedback by which the HS Heinrich Events in the North Atlantic initiate deglaciations [*Marchitto et al.*, 2007; *Sigman et al.*, 2007; *Anderson et al.*, 2009]. During and possibly just prior to HS Heinrich Events, perhaps resulting from insolation-driven melting of

---

[1]Alfred Wegener Institute for Polar and Marine Research, Department of Marine Geology and Paleontology, Bremerhaven, Germany.

[2]Leibniz Center for Earth Surface and Climate Studies, Institute for Geosciences, Potsdam University, Potsdam, Germany.

[3]CNR-IDPA Institute for the Dynamics of Environmental Processes and Department of Environmental Sciences, Informatics and Statistics, University Ca' Foscari of Venice, Venice, Italy.

[4]Godwin Laboratory for Palaeoclimate Research, Department of Earth Sciences, University of Cambridge, Cambridge, UK.

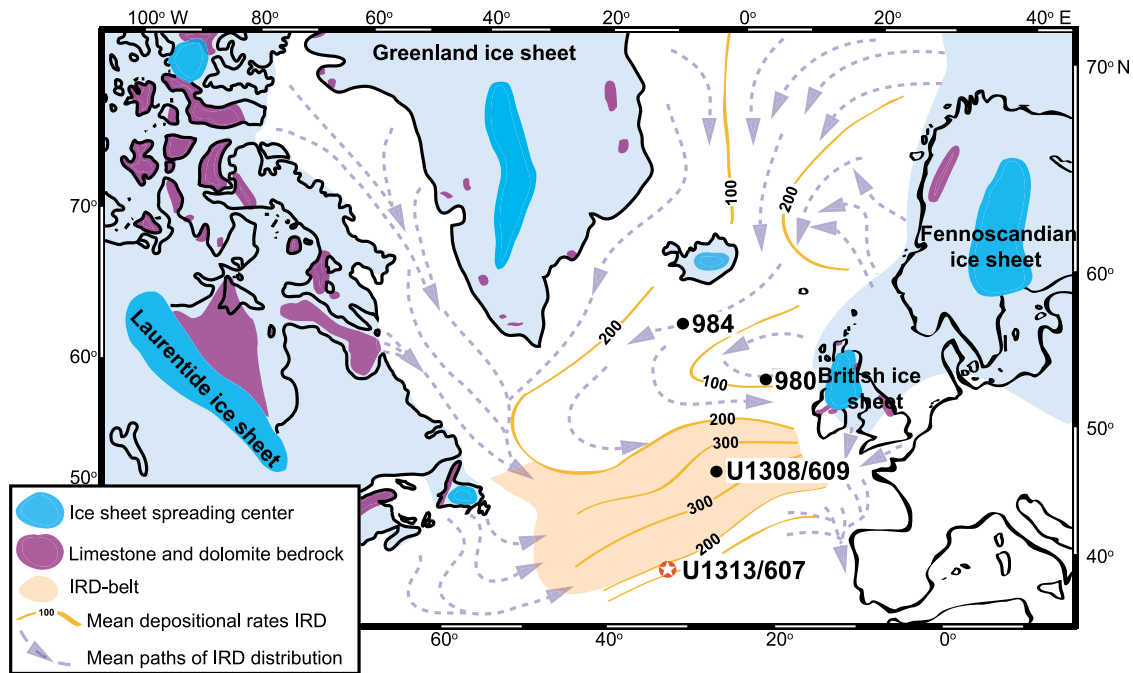[5]Geological Institute, ETH Zürich, Zurich, Switzerland.

Figure 1. Study area Map of the North Atlantic showing the location of IODP Site U1308 (re-drill of DSDP Site 609), IODP Site U1313 (re-drill of DSDP Site 607), and ODP Sites 980 and 984 together with the IRD accumulation for the last glacial period [*Ruddiman*, 1977]. The occurrence of Paleozoic carbonates around the North Atlantic, the source of dolomite, is highlighted with purple [*Bond et al.*, 1992]. This study uses samples from IODP Site U1313.

and/or internal instabilities in the Northern Hemisphere ice sheets [*Hemming*, 2004], North Atlantic overturning terminates [e.g., *McManus et al.*, 2004; *Pisias et al.*, 2010]. It has been suggested that this termination of North Atlantic overturning induced increased overturning and warming in the Southern Ocean [e.g., *Sigman et al.*, 2007; *Barker et al.*, 2009], yielding the observed abrupt rises in the Antarctic temperature and most likely atmospheric CO_2 [*Jouzel et al.*, 2007; *Lüthi et al.*, 2008]. Although the HS Heinrich Events thus appear to have been important during the last glacial termination and are the most dramatic examples of millennial-scale climate variability, little is known about the occurrence of HS Heinrich(-like) Events in older glacials especially when boundary conditions were different (e.g., across the Mid-Pleistocene Transition (MPT)).

[4] One recent study suggested that the occurrence of HS Heinrich(-like) Events at Integrated Ocean Drilling Program (IODP) Site U1308, a re-drill of DSDP Site 609 that played an important role for the discovery of Heinrich Events [e.g., *Bond et al.*, 1992; *Bond and Lotti*, 1995], was restricted to the "100-ka world" of the Pleistocene with the first HS Heinrich(-like) Event occurring during MIS 16 [*Hodell et al.*, 2008], the first prolonged glacial following the MPT [*Clark et al.*, 2006]. Although HS Heinrich(-like) Events were also found during MIS 16 at IODP Site U1313, this record ended at 650 ka [*Stein et al.*, 2009], so whether the onset of HS Heinrich(-like) Events at U1308 during MIS 16 represents a basin-wide signal remained unknown. More importantly, the possibility that the occurrence of HS Heinrich(-like) Events at U1308 was driven by a long-term decrease in SSTs in the eastern North Atlantic could not be ruled out [*Hodell et al.*, 2008]. Here we thus extended both the SST and IRD

record from IODP Site U1313 to 960 ka to investigate the correlation between the first occurrence of HS Heinrich(-like) Events and SSTs in the North Atlantic.

2. Study Material

[5] In this study sediment from IODP Site U1313 was used. Site U1313, a re-drill of Deep Sea Drilling Project (DSDP) Site 607, is located in the North Atlantic (latitude 41°00′N, longitude 32°57′W) at the southern boundary of the IRD-belt [*Ruddiman*, 1977] (Figure 1). At present Site U1313 is predominantly influenced by the warm and oligotrophic surface waters of the North Atlantic Current, leading to present-day mean annual SSTs of 18.3°C [*Locarnini et al.*, 2006]. During glacials however the surface water circulation in the North Atlantic was significantly different and colder conditions prevailed in the North Atlantic as the Arctic Front (AF) was located further south [*Pflaumann et al.*, 2003].

[6] During IODP Expedition 306 four holes were drilled at Site U1313 (3426 m water depth) from which two complete spliced stratigraphic sections for the Pleistocene were constructed [*Expedition 306 Scientists*, 2006]. Holes U1313B and U1313C were used for the primary splice, while U1313A and U1313D formed the secondary splice. The original meter composite depth (mcd)-scales from U1313A, U1313C, and U1313D were updated by tying them to the mcd-scale for Hole U1313B. Hereby an adjusted so-called amcd-scale was created that improved overall correlation of distinct features in the lightness, susceptibility, and paleomagnetic data between the holes (G. Acton, personal communication, 2010). For this study samples from the primary splice were used to obtain biomarker, XRD, and part of the foraminiferal
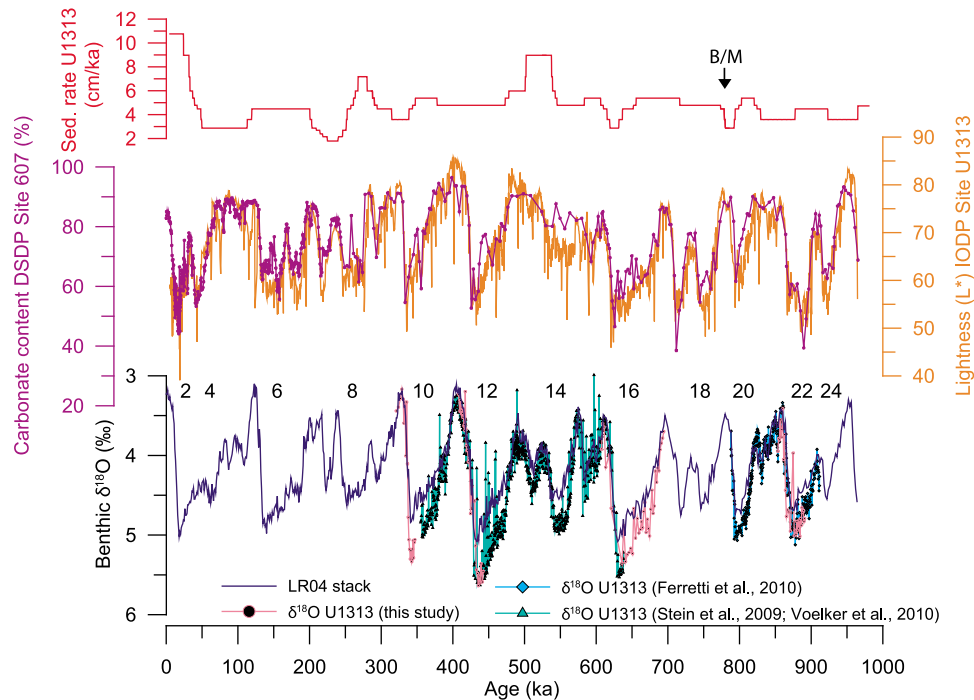
Figure 2. Chronology of Site U1313. Sedimentation rates at U1313 (red), carbonate content of DSDP Site 607 [*Ruddiman et al.*, 1989] (purple) together with lightness of the primary splice from U1313 (orange), and benthic $\delta^{18}O$ of Site U1313 [*Stein et al.*, 2009; *Ferretti et al.*, 2010; *Voelker et al.*, 2010; this study] together with the global benthic $\delta^{18}O$ stack [*Lisiecki and Raymo*, 2005]. Arrow with B/M indicates the position of the Bruhnes/Matuyama boundary.

$\delta^{18}O$ data. Samples from the secondary splice were used to reconstruct the Mg/Ca record and the remainder of the foraminiferal $\delta^{18}O$ data.

3. Chronology

[7] The chronology of Site U1313 between 14.5 and 46 amcd partly relies on benthic foraminiferal $\delta^{18}O$ data (Figure 2). In addition to the benthic foraminiferal $\delta^{18}O$ data from the secondary splice, which were previously published [*Stein et al.*, 2009; *Ferretti et al.*, 2010; *Voelker et al.*, 2010], we measured $\delta^{18}O$ on the benthic foraminifera *Cibicidoides wuellerstorfi* from Holes U1313B and U1313D across terminations IV, V, and X (4 cm sampling resolution) as well as during MIS 16 (10 cm sampling resolution). In total 123 new samples were measured.

[8] All benthic foraminiferal $\delta^{18}O$ data from U1313 for the interval between 960 and 320 ka were tuned to the LR04 stack [*Lisiecki and Raymo*, 2005]. At the same time the lightness of the primary splice (L*) from U1313 was tuned to the carbonate content of DSDP Site 607 [*Ruddiman et al.*, 1989], which is part of the LR04 stack. Lightness at Site U1313 is mainly controlled by variations in terrestrial input and is highly correlated with carbonate content at Site U1313 [*Stein et al.*, 2009]. The tuning was done using the Match 2.0 software [*Lisiecki and Lisiecki*, 2002]. Using our age model sedimentation rates vary between 2 and 10 cm/ka and the Bruhnes/Matuyama magnetic boundary is identified at 783 ka (Figure 2). The B/M boundary was not used as age-depth tie-point in order to give the Match 2.0 software more freedom to find the optimal correlation. Future high-

resolution studies from Site U1313 using a continuous benthic foraminiferal $\delta^{18}O$ record combined with paleo-intensities will undoubtedly improve this age model.

4. Methodology

4.1. Sea Surface Temperatures (SSTs)

[9] Mean annual SSTs were calculated using the alkenone unsaturation index ($U_{37}^{k\prime}$) and the global core top calibration [*Prahl and Wakeham*, 1987; *Müller et al.*, 1998]. The relative abundance (%) of the $C_{37:4}$ alkenone was used to reconstruct the influence of cold and less saline polar/arctic waters at Site U1313 [*Bendle et al.*, 2005].

4.2. Ice-Rafted Debris (IRD) Characteristics

[10] IRD was identified using X-Ray Diffraction (XRD) to distinguish material originating from different source areas. Quartz was used as a general proxy for continental-derived material, reflecting input from different circum-Atlantic ice sheets (e.g., Canadian Shield, Greenland, Scandinavia, Great Britain) [*Grousset et al.*, 2001; *Stein et al.*, 2009]. Following previous studies from the North Atlantic [e.g., *Andrews and Tedesco*, 1992; *Ji et al.*, 2009; *Stein et al.*, 2009] dolomite was used as an indicator for ice-rafted debris (IRD) originating from the Paleozoic carbonates in the Hudson area [*Bond et al.*, 1992] and thus HS Heinrich Events.

[11] In addition to the detrital component, Heinrich layers in the North Atlantic are characterized by an increased abundance of so-called petrogenic organic compounds that are normally absent in recent sediments. These include hopanes and steroids and their aromatic counterparts, as well

as palaerenieratane and isorenieratane and their derivatives, which indicate the input of ancient and organic rich material [*Rosell-Melé et al.*, 1997; *Rashid and Grosjean*, 2006]. Like the detrital component, the biomarker distribution points to a Paleozoic bedrock source in the Hudson area as the source for the organic material during Heinrich events [*Rashid and Grosjean*, 2006]. The most abundant petrogenic compound accumulating at Site U1313 during the four HS Heinrich events of the last glacial cycle is the $C_{28}(S)$ C-ring monoaromatic steroid. Although the exact mechanism for the formation of $C_{28}(S)$ C-ring monoaromatic steroids is not clear, it is an aromatization product of sterols (derived from eukaryotes) that forms during diagenesis. It is therefore normally absent in recent sediments, but common in source rocks and oils. The abundance of the $C_{28}(S)$ C-ring monoaromatic steroid was thus used as a proxy for the input of ancient and organic rich material and hence IRD.

5. Analytical Techniques

[12] Approximately 1500 sediment samples from the primary splice of Site U1313 were analyzed for biomarkers at the AWI-Bremerhaven using a LECO Pegasus III GC/TOF-MS system. Samples were taken at 2-cm resolution, corresponding to a temporal resolution of on average less then 500 years. Organic compounds were extracted from ±6 g of homogenized and freeze-dried sediment using dichloromethane and Automated Solvent Extraction (ASE 200, DIONEX, 5 min. at 100°C and 1000 psi). Total extracts were analyzed using a LECO Pegasus III (LECO Corp., St. Joseph, MI), interfaced to an Agilent 6890 GC. The gas chromatograph (GC) was equipped with a 15m x 0.18mm i.d. Rtx-1MS (Restek Corp., USA) column (film thickness: $0.10\mu m$) with an integrated 5 m guard column. The GC oven was initially held at 60°C for 1 min, then heated at 50°C min^{-1} to 250°C and at 30°C min^{-1} to 310°C (held 2.5 min), resulting in an analysis time of 9.3 min per sample.

[13] The occurrence and distribution of alkenones was monitored using the diagnostic *m/z* 94, 81, 79, 67, and 58 ionization fragments [*Hefter*, 2008]. A validated procedure was used to convert GC/TOF-MS C_{37} alkenone ratios to calibrated GC/FID values [*Hefter*, 2008]. The input of ancient and organic rich material was monitored using the diagnostic *m/z* 253 ionization fragment for C-ring monoaromatic steroids. Down core variations of the C_{28}S-triaromatic steroid are expressed semiquantitatively by normalizing the respective peak areas to the maximum area per gram sediment detected.

[14] XRD measurements were carried out at the AWI-Bremerhaven following the methods described by *Stein et al.* [2009], although here relative intensities of dolomite and quartz abundance were normalized to calcite. Between 660 and 320 ka, samples were measured for XRD at 2-cm (~500 years) resolution. For the remainder of the record, samples were measured for XRD at 10-cm (~2.5 ka) resolution, although during terminations a 2-cm (500 years) resolution was used to fully capture the IRD events.

[15] To obtain benthic foraminiferal $\delta^{18}O$ values, on average 5 specimens of *C. wuellerstorfi* were handpicked from the fraction larger than 250 μm and measured for $\delta^{18}O$ at the AWI-Bremerhaven, primarily using a Kiel carbonate device interfaced with a ThermoFinnigan MAT251 mass spectrometer. Some samples that contained only a few specimens

of *C. wuellerstorfi* were measured using a ThermoFinnigan MAT253 mass spectrometer, which needs less material. Analytical precision was 0.09 and 0.07‰ for $\delta^{18}O$ using the MAT251 and MAT253 mass spectrometer, respectively. $\delta^{18}O$ values were calibrated to the NBS-19 (National Bureau of Standards) and reported relative to the Vienna Pee Dee Belemnite (VPDB) standard. *C. wuellerstorfi* $\delta^{18}O$ was adjusted to equilibrium by adding 0.64‰.

[16] Paired measurements of Mg/Ca and $\delta^{18}O$ in planktonic foraminifera were predominantly performed in samples from the secondary splice of Site U1313. *G. ruber* was selected from the larger than 250 μm coarse fraction of sediment samples. Around 20 *G. ruber* specimens per sample were measured for $\delta^{18}O$ at the AWI-Bremerhaven. *G. bulloides* was selected from the 315–355 μm coarse fraction of sediment samples, and on average 80 specimens were picked for isotope and minor element analyses in order to reduce statistical variability. All $\delta^{18}O$ and minor element analyses on *G. bulloides* were carried out at the Analytical Service Unit of the University of Barcelona using a ThermoFinnigan MAT 252 mass spectrometer linked online to a single acid bath CarboKiel-II carbonate preparation device and a Perkin Elmer Elan 6000 quadrupole ICP-MS respectively. The Mg/Ca cleaning process is after *Pena et al.* [2005] and involved the following steps. 1) Clay removal: crushed samples were rinsed and briefly ultrasonicated in ultrahigh quality water (UHQ H_2O) five times, in methanol (Aristar grade) twice, and then in UHQ H_2O again to remove clays and fine-grained carbonates. 2) Reductive cleaning: to remove a variety of contaminants phases, such as Mn-Fe oxides, a reductive reagent composed by a mixture of hydrazine hydroxide, citric acid and ammonia hydroxide was used in a hot (c. 100°C) ultrasonic bath for fifteen minutes with brief intervals of ultrasonication, followed by rinsing. 3) Oxydative cleaning: to remove organic matter, samples were then reacted with an oxidizing reagent (alkali buffered (NaOH) hydrogen peroxide (H_2O_2) 1% solution) in a boiling water bath for ten minutes with brief intervals of ultrasonication, followed by rinsing. 4) Samples were then checked under the microscope for coarse grained-silicates and any particles that were not apparently carbonate were removed using a fine brush. 5) Weak acid leach: to remove any remaining contaminant phase or particle that could be still attached to the foraminifera walls, samples were reacted with a weak acid (0.001 M HNO_3) and were rinsed in UHQ H_2O. 6) Finally, cleaned samples were dissolved the day of analysis in ultrapure HNO3 (1%), ultrasonicated to promote dissolution, centrifuged in order to settle out any of the less soluble impurities, and then transferred to clean vials to prevent possible leaching from residual particles. Mg/Ca ratios were converted to temperatures using the calibration from *Elderfield and Ganssen* [2000].

6. Results

[17] Based on the increased abundance of dolomite and $C_{28}(S)$ C-ring monoaromatic steroids during the last glacial cycle, HS Heinrich Events 1, 2, 4, and 5 can easily be identified at Site U1313 (Figure 3). Heinrich Events 3 and 6 are absent in the dolomite/calcite record, suggesting that no IRD from the LIS reached the study location in the eastern North Atlantic during these events.
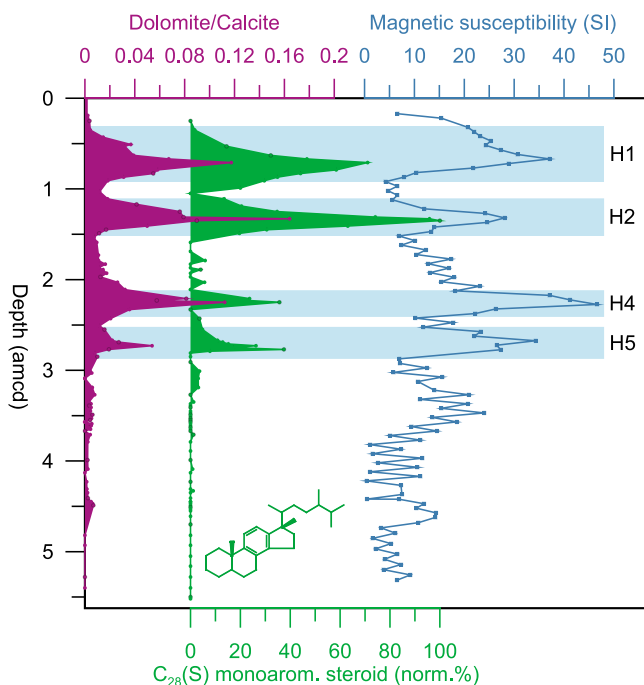
Figure 3. Dolomite and $C_{28}(S)$ abundance during the most recent glacial cycle. Dolomite/calcite (purple), relative abundance of the monoaromatic steroid $C_{28}(S)$ (green), and magnetic susceptibility (blue) at Site U1313 for the upper 5 amcd. Dolomite/calcite and $C_{28}(S)$ abundance are high during Heinrich layers 1, 2, 4, and 5; the four HS Heinrich events [*Hemming*, 2004].

[18] For the period between 960 and 320 ka, periods of increased quartz deposition characterize glacials, especially glacial terminations (Figure 4h). These events are associated with severe cooling of surface waters and expansion of arctic/polar waters into the midlatitude North Atlantic (Figures 4d and 4e). During glacial terminations (TX, TVIII, and TIV), minima in SSTs occasionally lag benthic foraminiferal $\delta^{18}O$ by several ka (Figure 5). Dolomite/calcite is below or just above detection limits prior to MIS 16. At 643 ka (MIS 16) dolomite becomes abundant for the first time in the sediment, followed by high abundance during termination VII. After MIS 16, dolomite became abundant in the sediment during the later stages of MIS 12 and 10, but remained low during MIS 14 [*Stein et al.*, 2009]. The abundance of the $C_{28}(S)$ C-ring monoaromatic steroid is highly correlated with the occurrence of dolomite, not only during the last glacial cycle (Figure 3), but also throughout the period between 960 and 320 ka (Figures 4f and 4g). The $C_{28}(S)$ C-ring monoaromatic steroid was thus absent before MIS 16 and abundant during the later stages of MIS 16, 12, and 10.

[19] The high-resolution (0.4 ka resolution) alkenone-based SST record shows that for most of our record, SSTs follow the typical glacial/interglacial pattern with SSTs of around 19°C during interglacials and as low as 8°C during IRD-events. Lowest SSTs are found during MIS 12 and 10. However, MIS 16 stands out as a glacial with SSTs steadily increasing to values as high as 16°C, opposite to the increasing trend in ice volume (Figures 4c and 4d). Only

during TVII did SSTs drop again to lower values. High-latitude waters were also absent at Site U1313 during MIS 16 as almost no $C_{37:4}$ alkenones were found in the sediment during this glacial (Figure 4e).

7. Discussion

7.1. Occurrence of HS Heinrich(-like) Events

[20] The lack of dolomite prior to MIS 16 indicates that no IRD from the Hudson area was deposited at Site U1313 and hence suggests the absence of HS Heinrich(-like) Events prior to MIS 16. At 643 ka (MIS 16) the increased abundance of dolomite indicates the first HS Heinrich(-like) Events at Site U1313. The first HS Heinrich(-like) Event in the sedimentary record was shortly followed by a second HS Heinrich(-like) Event that coincides with termination VII. Following MIS 16, HS Heinrich(-like) Events occurred during the later stages of MIS 12 and 10 [*Stein et al.*, 2009]. All these HS Heinrich Events were also characterized by the input of ancient and organic rich material, possibly originating from the Hudson area, as indicated by the increased abundance of the $C_{28}(S)$ C-ring monoaromatic steroid. In addition, despite the uncertainties in age models all these HS Heinrich(-like) Events coincide with periods of rising CO_2 (Figure 4), suggesting that the feedback mechanisms in the Southern Hemisphere associated with the HS Heinrich Events of the last glacial cycle [e.g., *Sigman et al.*, 2007] were also present during older glacials.

[21] The timing of the HS Heinrich(-like) Events at U1313 agrees with results from Site U1308 where HS Heinrich(-like) Events were also detected during MIS 16, 12, and 10, but were absent in older glacials [*Hodell et al.*, 2008]. The synchrony between these two sites across the IRD-belt indicates that the onset of HS Heinrich(-like) Events was simultaneous within the (eastern) North Atlantic. More over the synchrony suggests that these events can be traced throughout the (eastern) North Atlantic and we therefore propose to uniformly name the HS Heinrich(-like) Events according to the glacial and order they occur. In this way the HS Heinrich(-like) Events that occurred during the glacial terminations, also referred to as terminal ice rafting events [*Venz et al.*, 1999], are labeled HS Heinrich(-like) Event 16.1, 12.1, and 10.1 (Figure 4).

7.2. Sea Surface Temperatures

[22] The alkenone-based SST record shows that SSTs did not cause the first occurrence of HS Heinrich(-like) Events. Alkenone-based SSTs at Site U1313 were higher during the onset of HS Heinrich(-like) Events (MIS 16) than during other glacials. This is surprising as during all other glacials, a part from the weak glacial of MIS 14, SSTs at Site U1313 indicate significant cooling of surface waters, especially during ice-rafting events as melting icebergs filled the North Atlantic. Although during the HS Heinrich(-like) Event of termination VII (16.1) SSTs at Site U1313 also depict the influence of the melting of icebergs, SSTs remain higher than during other glacials. A lower resolution record of summer and winter SSTs based on census counts of planktonic foraminifera from Site 607 [*Ruddiman et al.*, 1989], of which U1313 is a re-drill, shows the same warming trend during MIS 16. These SSTs thus confirm the higher resolution alkenone-based SSTs during MIS 16 (Figure 6a). The small
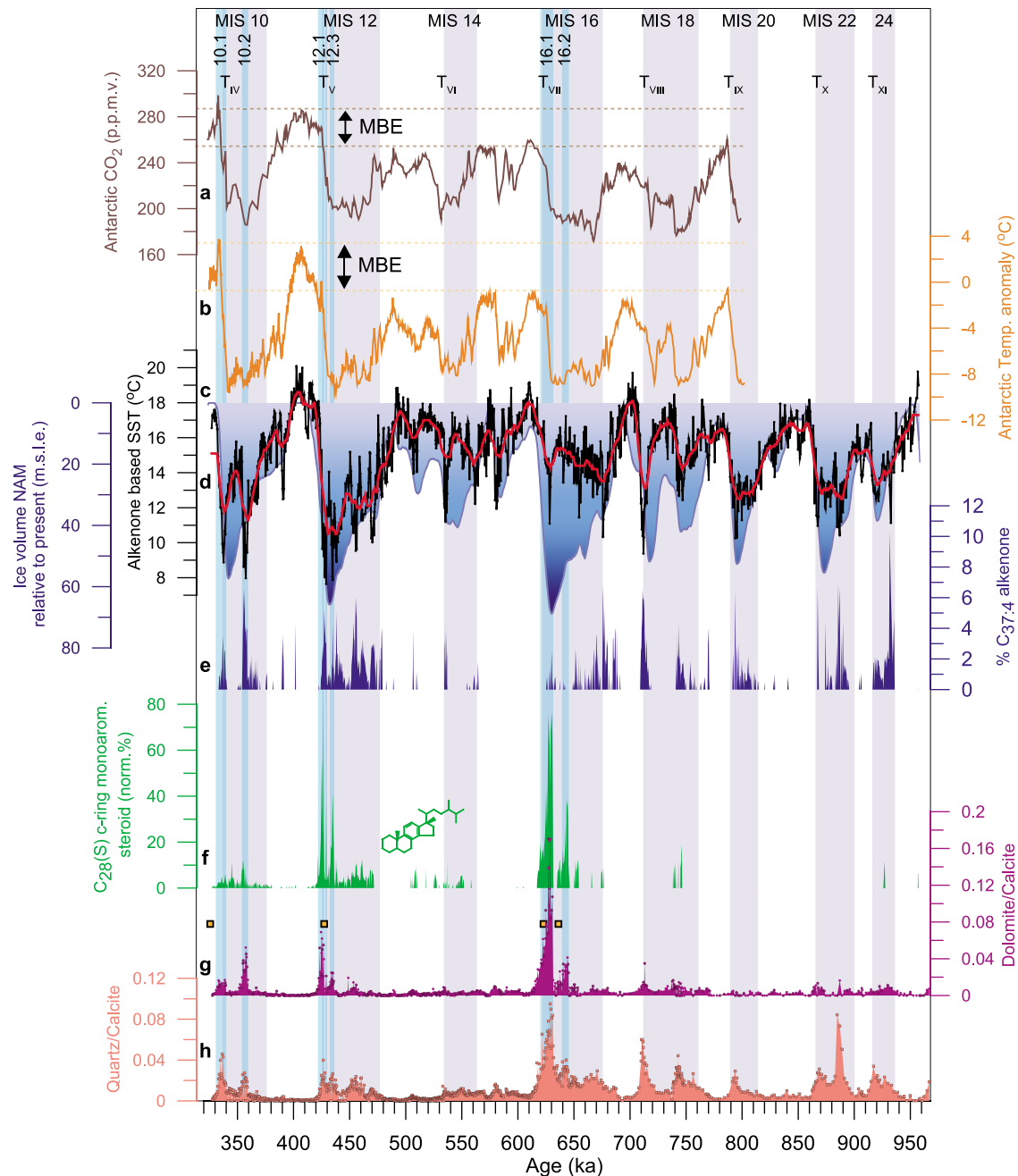
Figure 4. Multiproxy records of IODP Site U1313 between 960 and 320 ka. (a) Atmospheric CO_2-levels, reconstructed from Antarctic ice cores [*Lüthi et al.*, 2008]. (b) Antarctic air temperature anomaly [*Jouzel et al.*, 2007]. (c) Modeled size of the North American ice sheets, based on benthic foraminiferal $\delta^{18}O$ [*Bintanja and van de Wal*, 2008]. (d) High-resolution alkenone-based SST (black) and 10-ka moving average (thick red line). (e) Abundance of $C_{37:4}$ alkenones, indicative of high-latitude waters. (f) Relative abundance of the $C_{28}(S)$ c-ring monoaromatic steroid, indicative for the input of ancient and organic rich material. (g) Abundance of dolomite, indicative for the input of IRD from the Hudson Bay area. (h) Abundance of quartz, indicative for the input of IRD from circum-Atlantic ice sheets. Light blue bars indicate the occurrence of HS Heinrich(-like) Events at Site U1313. Grey bars highlight glacials. Orange cubes indicate the timing of HS Heinrich(-like) Events at IODP Site U1308 [*Hodell et al.*, 2008]. The occurrence of the Mid-Brunhes Event (MBE) is indicated by black arrows in Figures 4a and 4b.
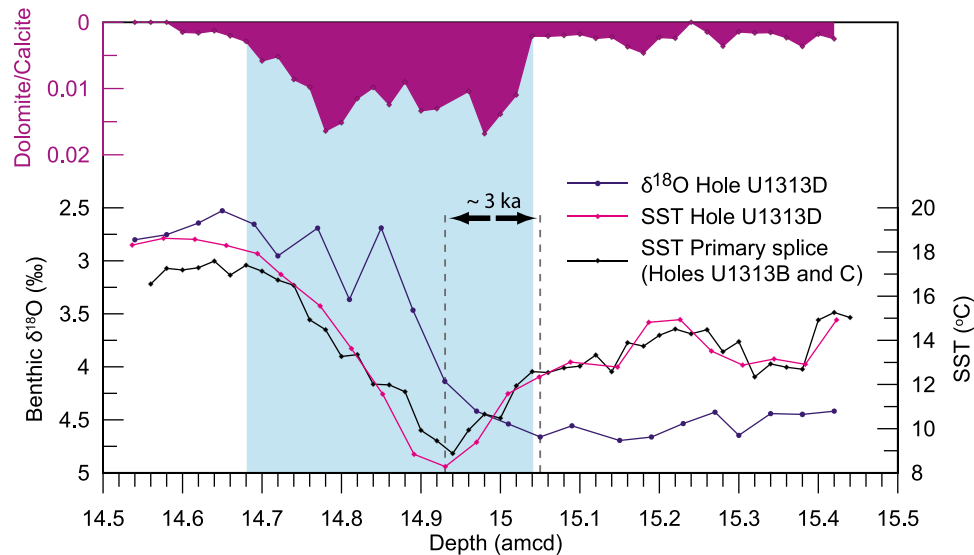
Figure 5. Termination IV Benthic foraminiferal δ^{18}O (blue) and alkenone-based SSTs (pink) from samples from Hole U1313D together with alkenone-based SSTs from the primary splice (black), formed from Holes U1313B and U1313C, versus depth. Minima in SSTs lag maxima in benthic foraminiferal δ^{18}O by 12 cm, which corresponds to ~3 ka using our age model. Dolomite/calcite (purple) is shown to indicate the occurrence of HS Heinrich(-like) Event 10.1 (blue bar).

temporal offset between the SST records from Site U1313 and Site 607 is probably related to the difference in resolution and age models.

[23] The occasional lag between minima in SSTs and maxima in benthic foraminiferal δ^{18}O during glacial terminations demonstrates the impact of ice-rafting events on surface water characteristics in the North Atlantic during the Pleistocene as the meltwater pulse for a short period suppressed the warming of surface waters to interglacial values. This is especially evident during termination IV (Figure 5). It is important to note that the timing of these ice-rafting events and associated cooling of surface waters at Site U1313 is different compared to those at the Iberian Margin were maximum IRD input preceded minima in SSTs [*Rodrigues et al.*, 2011] and minima in SSTs coincide with maxima in benthic foraminiferal δ^{18}O during termination IV [*Martrat et al.*, 2007; *Rodrigues et al.*, 2011]. As IRD at the Iberian Margin is thought to have various sources, including the European ice sheets [*de Abreu et al.*, 2003; *Bigg et al.*, 2010], the difference between Site U1313 and Iberian Margin could indicate an offset in the timing of the collapse of the European and Laurentide ice sheets. In addition, this apparent difference between the midlatitude North Atlantic and Iberian Margin urges for care in correlating IRD-events across the North Atlantic.

7.3. Stratification of the Water Column

[24] To investigate whether the warming of surface waters during MIS 16 was restricted to the upper part of the water column, Mg/Ca in the planktonic foraminifera *Globigerina bulloides* was measured. *G. bulloides* is a mixed-layer-dwelling planktonic foraminifera, which in the North Atlantic can be found throughout the upper 60 m of the water column [*Schiebel et al.*, 1997]. The Mg/Ca record thus represents a shallow subsurface temperature signal, while

alkenone-based SSTs are thought to represent temperatures of the upper 10 m of the water column [*Müller et al.*, 1998].

[25] The results show that Mg/Ca based temperatures were decreasing during MIS 16, opposite to the trends in the alkenone-based and census counts of planktonic foraminifera based SSTs (Figure 6b). The difference between the alkenone- and Mg/Ca-based SSTs reaches up to 6°C during MIS 16, while the two temperature records show similar values during the interglacials MIS 17 and 15. This indicates a large temperature gradient between the upper-part of the water column (alkenone-based SSTs) and underlying waters (Mg/Ca-based SSTs) during MIS 16. We interpret this increased temperature gradient to reflect a strong stratification of the water column. This is also supported by the increased offset in δ^{18}O between *G. bulloides* and the surface-dwelling planktonic foraminifera *Globigerinoides ruber* that doubled during MIS 16 (Figures 6c and 6d).

[26] The possibility that the difference between alkenone- and planktonic foraminiferal δ^{18}O-based SSTs reflects amplification of seasonal differences as was proposed for the North Pacific [*Haug et al.*, 2005] is unlikely to play a major role at our study site. In the North Atlantic *G. ruber*, *G. bulloides* and coccolithophores, of which a small group produces alkenones, all bloom in (late) spring [*Weeks et al.*, 1993; *Elderfield and Ganssen*, 2000; *Ganssen and Kroon*, 2000; *Chapman*, 2010]. In addition, alkenone-based SSTs during MIS 16 remain between the seasonal extremes as determined by summer and winter SSTs based on census counts of foraminifera from Site 607 [*Ruddiman et al.*, 1989] and thus do not indicate a shift toward summer temperatures. At the same time, Mg/Ca-based temperatures during MIS 16 are lower than the reconstructed winter SSTs, again suggesting that the Mg/Ca record represents shallow subsurface temperatures.
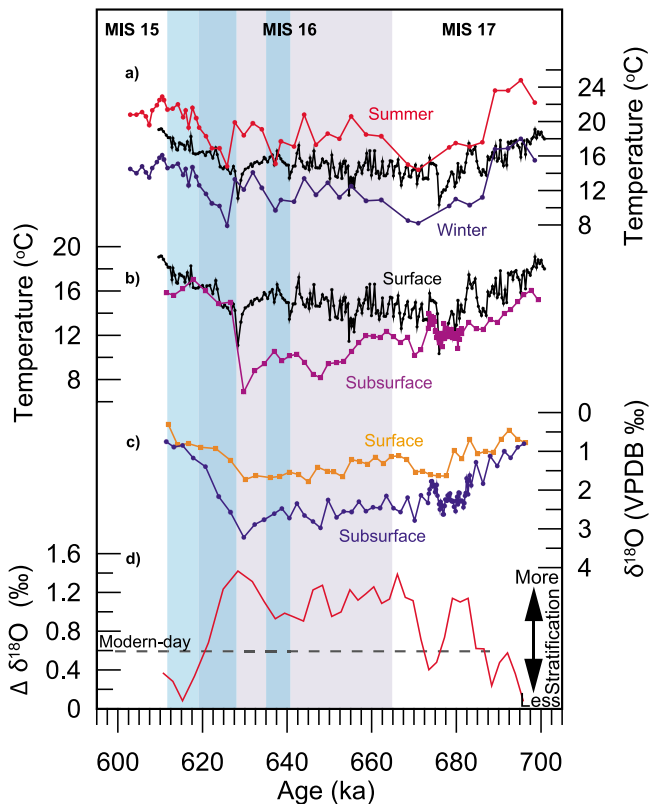
Figure 6. MIS 16. (a) Alkenone-based annual mean SSTs from U1313 (black) and foraminiferal assemblage-based summer (red) and winter (dark blue) SST from DSDP Site 607 [*Ruddiman et al.*, 1989], of which U1313 is a re-drill. (b) Alkenone-based SSTs from U1313 (black) together with shallow subsurface temperature estimates at U1313, based on Mg/Ca from the mixed-layer-dwelling planktonic foraminifera *G. bulloides* (purple). (c) Planktonic foraminiferal δ^{18}O of the surface-dwelling *G. ruber* (orange) and mixed-layer-dwelling *G. bulloides* (blue). (d) Difference in δ^{18}O between *G. bulloides* and *G. ruber*. Dashed line indicates the present-day offset [*Ganssen and Kroon*, 2000]. Color bars are like in Figure 4.

7.4. Cause for Warm SSTs During MIS 16

[27] We interpret the warm and stratified surface waters at Site U1313 to reflect a more northern position of the Arctic Front (AF) during MIS 16, more comparable to interglacial than to glacial conditions. A more northern position of the AF is also supported by foraminiferal data from Ocean Drilling Project (ODP) Sites 984 and 980 that indicate a northward movement of the AF during MIS 16 [*Wright and Flower*, 2002]. Within the North Atlantic, the AF is characterized by a steep SST gradient and forms the boundary between warm Atlantic waters and cold arctic waters [*Swift*, 1986]. During the last glacial maximum the southern location of the AF between 45 and 37°N led to a strong SST gradient in the midlatitude North Atlantic with warm surface waters accumulating directly south of the AF [*Pflaumann et al.*, 2003]. Previous results suggested that a slightly more northern position of the AF during MIS 6 led to higher SSTs in the midlatitude North Atlantic [*Calvo et al.*, 2001].

A more northerly position of the AF during MIS 16 compared to other glacials could thus explain the higher SSTs at Site U1313.

[28] Today, North Atlantic deep water formation establishes the upper ocean and atmospheric circulation that ameliorates the climate of the eastern circum-North Atlantic [*Rahmstorf*, 2002]. The moderate North Atlantic SSTs of MIS 16 due to a more northerly position of the AF thus suggest greater North Atlantic overturning at that time as compared to other glacials. The ultimate cause for this different ocean circulation in the North Atlantic remains unknown. Possibly the increased input of warm and salty waters by means of Agulhas Leakage during MIS 16, compared to MIS 12 and 10, promoted the greater overturning in the North Atlantic [*Bard and Rickaby*, 2009]. However, this does not explain why glacials prior to MIS 16 were characterized by low SSTs in the North Atlantic as the Agulhas Leakage during these glacials was comparable to MIS 16 [*Bard and Rickaby*, 2009]. Future research should therefore focus on the ultimate mechanisms behind the different ocean circulation in the North Atlantic during MIS 16.

7.5. Implications

[29] The results presented here confirm the previous suggestion that MIS 16 marks a change in LIS dynamics, possibly due to an increases in LIS ice volume (thickness), as HS Heinrich Events appeared in the sedimentary record of the eastern North Atlantic [*Hodell et al.*, 2008]. This agrees with recent results of ice sheet modeling [*Bintanja and van de Wal*, 2008] and dating of glacial stratigraphic sections in North America [*Roy et al.*, 2004; *Balco and Rovey*, 2010] which suggested that the size and volume of the North American ice sheets increased at the end of the early Pleistocene and highlighted the role of ice sheets, in particular the North American ice sheets, in the MPT [*Bintanja and van de Wal*, 2008].

[30] In addition, in the context of the feedback mechanisms associated with HS Heinrich Events by which the North Atlantic initiates dramatic deglaciations [*Marchitto et al.*, 2007; *Sigman et al.*, 2007; *Anderson et al.*, 2009], our results add to the data suggesting a correlation between the occurrence of HS Heinrich(-like) Events and the stronger interglacials that characterize the Pleistocene after the Mid-Brunhes Event (MBE) at ~450 ka. The MBE is the most obvious in the Antarctic ice core records of CO_2 and temperature (Figures 4a and 4b), but can also be found in other climate records from around the world as a shift toward more intense interglacial conditions [*Lang and Wolff*, 2010]. Specifically the first strong interglacial defining the MBE is preceded by the HS Heinrich(-like) Events of MIS 12 while, with the exception of MIS 15, the earlier "luke-warm" interglacials (MIS 19–13) with weaker deglacial increases in Antarctic temperature [*Jouzel et al.*, 2007] and CO_2-levels [*Lüthi et al.*, 2008], did not have preceding HS Heinrich(-like) Events.

[31] The major exception to the rule is thus MIS 16, which did have HS Heinrich(-like) Events but even so was followed by the luke-warm interglacial MIS 15 (Figures 4a and 4b). This suggests an additional requirement for the dramatic deglaciations that characterize the latest Pleistocene. Our alkenone temperature reconstructions may provide an additional insight into this. Despite the intensity of the MIS 16,

unusually moderate North Atlantic SSTs characterized this period possible due to substantial North Atlantic overturning. The hypothesized North-to-South trigger for deglaciations revolves around the shutdown of North Atlantic overturning [*Sigman et al.*, 2007; *Anderson et al.*, 2009]. In a glacial with strong North Atlantic overturning (e.g., MIS 16), even a HS Heinrich(-like) Event may not have been adequate to cause this shut-down. That is, the data from stage 16 may be indicating that the HS Heinrich Event trigger can only work in glacial states with already weak and/or shallow North Atlantic overturning.

8.   Conclusion

[32]   Our high-resolution records depict the detailed relation between surface water characteristics and IRD-events in the midlatitude North Atlantic for the period between 960 and 320 ka. The IRD-characteristics demonstrate that although regular IRD-events occurred throughout this interval, predominantly during glacial terminations, IRD originating from the Laurentide Ice sheet and thus HS Heinrich(-like) Events was absent prior to MIS 16. During IRD-events SSTs indicate severe cooling of surface waters and increased influence of high-latitude waters. At 643 ka, dolomite for the first time became abundant and indicates the first occurrence of HS Heinrich(-like) Events. Following MIS 16, HS Heinrich(-like) Events occurred during MIS 12 and 10. All these events are characterized by the input of ancient and organic rich material. The timing of these events is similar as at Site U1308, located further to the North, and indicates a simultaneous onset within the (eastern) North Atlantic.

[33]   The alkenone-based SST record shows the first occurrence was not simply related to increased survivability, as SSTs were significantly higher during MIS 16 than during other glacials, probably due to a more northern location of the AF. Lower subsurface temperature estimates based on Mg/Ca from mixed-layer dwelling planktonic foraminifera suggest that the warming was restricted to the upper part of the water column. These results indicate that MIS 16 marks a change in LIS dynamics, in-line with previous studies. This has large implications for the role of HS Heinrich(-like) Events within the broader climate system as the results of HS Heinrich(-like) Events occurring prior to the MBE suggest that the occurrence of HS Heinrich events alone is not enough to initiate dramatic deglaciations, and other mechanisms might be needed to reach the full interglacial conditions that characterize the last 450 ka.

[34]   The next step will now be to determine the onset of HS Heinrich(-like) Events in the sedimentary record close to the source area (e,g, Labrador Sea), where even small ice-rafting events can be detected that would not influence the eastern North Atlantic.

References

Anderson, R. F., S. Ali, L. I. Bradtmiller, S. H. H. Nielsen, M. Q. Fleisher, B. E. Anderson, and L. H. Burckle (2009), Wind-Driven Upwelling in the Southern Ocean and the Deglacial Rise in Atmospheric CO_2, *Science*, *323*(5920), 1443–1448, doi:10.1126/science.1167441.

Andrews, J. T., and K. Tedesco (1992), Detrital carbonate-rich sediments, northwestern Labrador Sea: Implications for ice-sheet dynamics and iceberg rafting (Heinrich) events in the North Atlantic, *Geology*, *20*(12), 1087–1090, doi:10.1130/0091-7613(1992)020<1087:DCRSNL>2.3.CO;2.

Balco, G., and C. W. Rovey (2010), Absolute chronology for major Pleistocene advances of the Laurentide Ice Sheet, *Geology*, *38*(9), 795–798, doi:10.1130/G30946.1.

Bard, E., and R. E. M. Rickaby (2009), Migration of the subtropical front as a modulator of glacial climate, *Nature*, *460*(7253), 380–383, doi:10.1038/nature08189.

Bard, E., F. Rostek, J.-L. Turon, and S. Gendreau (2000), Hydrological impact of Heinrich Events in the subtropical northeast Atlantic, *Science*, *289*(5483), 1321–1324, doi:10.1126/science.289.5483.1321.

Barker, S., P. Diz, M. J. Vautravers, J. Pike, G. Knorr, I. R. Hall, and W. S. Broecker (2009), Interhemispheric Atlantic seesaw response during the last deglaciation, *Nature*, *457*(7233), 1097–1102, doi:10.1038/nature07770.

Bendle, J., A. Rosell-Melé, and P. Ziveri (2005), Variability of unusual distributions of alkenones in the surface waters of the Nordic seas, *Paleoceanography*, *20*, PA2001, doi:10.1029/2004PA001025.

Bigg, G. R., R. C. Levine, C. D. Clark, S. L. Greenwood, H. Haflidason, A. L. C. Hughes, A. Nygård, and H. P. Sejrup (2010), Last glacial ice-rafted debris off southwestern Europe: The role of the British-Irish Ice Sheet, *J. Quat. Sci.*, *25*(5), 689–699, doi:10.1002/jqs.1345.

Bintanja, R., and R. S. W. van de Wal (2008), North American ice-sheet dynamics and the onset of 100,000-year glacial cycles, *Nature*, *454*(7206), 869–872, doi:10.1038/nature07158.

Bond, G. C., and R. Lotti (1995), Iceberg Discharges into the North Atlantic on Millennial Time Scales During the Last Glaciation, *Science*, *267*(5200), 1005–1010, doi:10.1126/science.267.5200.1005.

Bond, G., et al. (1992), Evidence for massive discharges of icebergs into the North Atlantic ocean during the last glacial period, *Nature*, *360*(6401), 245–249, doi:10.1038/360245a0.

Broecker, W., G. Bond, M. Klas, E. Clark, and J. McManus (1992), Origin of the northern Atlantic's Heinrich events, *Clim. Dyn.*, *6*, 265–273, doi:10.1007/BF00193540.

Calvo, E., J. Villanueva, J. O. Grimalt, A. Boelaert, and L. Labeyrie (2001), New insights into the glacial latitudinal temperature gradients in the North Atlantic. Results from $U^{K'}_{37}$ sea surface temperatures and terrigenous inputs, *Earth Planet. Sci. Lett.*, *188*(3–4), 509–519, doi:10.1016/S0012-821X(01)00316-8.

Chapman, M. R. (2010), Seasonal production patterns of planktonic foraminifera in the NE Atlantic Ocean: Implications for paleotemperature and hydrographic reconstructions, *Paleoceanography*, *25*, PA1101, doi:10.1029/2008PA001708.

Clark, P. U., et al. (2006), The middle Pleistocene transition: Characteristics, mechanisms, and implications for long-term changes in atmospheric pCO2, *Quat. Sci. Rev.*, *25*(23–24), 3150–3184, doi:10.1016/j.quascirev.2006.07.008.

de Abreu, L., N. J. Shackleton, J. Schönfeld, M. Hall, and M. Chapman (2003), Millennial-scale oceanic climate variability off the Western Iberian margin during the last two glacial periods, *Mar. Geol.*, *196*(1–2), 1–20, doi:10.1016/S0025-3227(03)00046-X.

Elderfield, H., and G. Ganssen (2000), Past temperature and δ18O of surface ocean waters inferred from foraminiferal Mg/Ca ratios, *Nature*, *405*(6785), 442–445, doi:10.1038/35013033.

Expedition 306 Scientists (2006), Site U1313, in *North Atlantic Climate 1*, edited by J. E. T. Channell et al., *Proc. Integrated Ocean Drill. Program*, 303, doi:10.2204/iodp.proc.303306.112.2006.

Ferretti, P., S. J. Crowhurst, M. A. Hall, and I. Cacho (2010), North Atlantic millennial-scale climate variability 910 to 790 ka and the role of the equatorial insolation forcing, *Earth Planet. Sci. Lett.*, *293*, 28–41, doi:10.1016/j.epsl.2010.02.016.

Ganssen, G. M., and D. Kroon (2000), The isotopic signature of planktonic foraminifera from NE Atlantic surface sediments: Implications for the

reconstruction of past oceanic conditions, *J. Geol. Soc.*, *157*(3), 693–699, doi:10.1144/jgs.157.3.693.

Grousset, F. E., L. Labeyrie, J. A. Sinko, M. Cremer, G. Bond, J. Duprat, E. Cortijo, and S. Huon (1993), Patterns of ice-rafted detritus in the glacial North Atlantic (40–55°N), *Paleoceanography*, *8*(2), 175–192, doi:10.1029/92PA02923.

Grousset, F. E., E. Cortijo, S. Huon, L. Hervè, T. Richter, D. Burdloff, J. Duprat, and O. Weber (2001), Zooming in on Heinrich Layers, *Paleoceanography*, *16*(3), 240–259, doi:10.1029/2000PA000559.

Gwiazda, R. H., S. R. Hemming, and W. S. Broecker (1996), Provenance of icebergs during Heinrich Event 3 and the contrast to their sources during other Heinrich episodes, *Paleoceanography*, *11*(4), 371–378, doi:10.1029/96PA01022.

Haug, G. H., et al. (2005), North Pacific seasonality and the glaciation of North America 2.7 million years ago, *Nature*, *433*(7028), 821–825, doi:10.1038/nature03332.

Hefter, J. (2008), Analysis of alkenone unsaturation indices with fast gas chromatography/time-of-flight mass spectrometry, *Anal. Chem.*, *80*(6), 2161–2170, doi:10.1021/ac702194m.

Heinrich, H. (1988), Origin and consequences of cyclic ice rafting in the northeast Atlantic Ocean during the past 130,000 years, *Quat. Res.*, *29*(2), 142–152, doi:10.1016/0033-5894(88)90057-9.

Hemming, S. R. (2004), Heinrich events: Massive late Pleistocene detritus layers of the North Atlantic and their global climate imprint, *Rev. Geophys.*, *42*, RG1005, doi:10.1029/2003RG000128.

Hodell, D. A., J. E. T. Channell, J. H. Curtis, O. E. Romero, and U. Röhl (2008), Onset of "Hudson Strait" Heinrich events in the eastern North Atlantic at the end of the middle Pleistocene transition (~640 ka)?, *Paleoceanography*, *23*, PA4218, doi:10.1029/2008PA001591.

Ji, J., Y. Ge, W. Balsam, J. E. Damuth, and J. Chen (2009), Rapid identification of dolomite using a Fourier Transform Infrared Spectrophotometer (FTIR): A fast method for identifying Heinrich events in IODP Site U1308, *Mar. Geol.*, *258*(1–4), 60–68, doi:10.1016/j.margeo.2008.11.007.

Jouzel, J., et al. (2007), Orbital and Millennial Antarctic Climate Variability over the Past 800,000 Years, *Science*, *317*(5839), 793–796, doi:10.1126/science.1141038.

Lang, N., and E. W. Wolff (2010), Interglacial and glacial variability from the last 800 ka in marine, ice and terrestrial archives, *Clim. Past Discuss.*, *6*(5), 2223–2266, doi:10.5194/cpd-6-2223-2010.

Lisiecki, L. E., and P. A. Lisiecki (2002), Application of dynamic programming to the correlation of paleoclimate records, *Paleoceanography*, *17*(4), 1049, doi:10.1029/2001PA000733.

Lisiecki, L. E., and M. E. Raymo (2005), A Pliocene-Pleistocene stack of 57 globally distributed benthic $\delta^{18}O$ records, *Paleoceanography*, *20*, PA1003, doi:10.1029/2004PA001071.

Locarnini, R. A., A. V. Mishonov, J. I. Antonov, T. P. Boyer, and H. E. Garcia (2006), *World Ocean Atlas 2005*, vol. 1, *Temperature*, *NOAA Atlas NESDIS*, vol. 61, edited by S. Levitus, 182 pp., NOAA, Silver Spring, Md.

Lüthi, D., et al. (2008), High-resolution carbon dioxide concentration record 650,000–800,000 years before present, *Nature*, *453*(7193), 379–382, doi:10.1038/nature06949.

Marchitto, T. M., S. J. Lehman, J. D. Ortiz, J. Flückiger, and A. van Geen (2007), Marine radiocarbon evidence for the mechanism of deglacial atmospheric CO_2 rise, *Science*, *316*(5830), 1456–1459, doi:10.1126/science.1138679.

Martrat, B., J. O. Grimalt, N. J. Shackleton, L. de Abreu, M. A. Hutterli, and T. F. Stocker (2007), Four climate cycles of recurring deep and surface water destabilizations on the Iberian Margin, *Science*, *317*(5837), 502–507, doi:10.1126/science.1139994.

McManus, J. F., R. F. Anderson, W. S. Broecker, M. Q. Fleisher, and S. M. Higgins (1998), Radiometrically determined sedimentary fluxes in the sub-polar North Atlantic during the last 140,000 years, *Earth Planet. Sci. Lett.*, *155*(1–2), 29–43, doi:10.1016/S0012-821X(97)00201-X.

McManus, J. F., R. Francois, J. M. Gherardi, L. D. Keigwin, and S. Brown-Leger (2004), Collapse and rapid resumption of Atlantic meridional circulation linked to deglacial climate changes, *Nature*, *428*(6985), 834–837, doi:10.1038/nature02494.

Müller, P. J., G. Kirst, G. Ruhland, I. von Storch, and A. Rosell-Melé (1998), Calibration of the alkenone paleotemperature index Uk′37 based on core-tops from the eastern South Atlantic and the global ocean (60°N–60°S), *Geochim. Cosmochim. Acta*, *62*(10), 1757–1772, doi:10.1016/S0016-7037(98)00097-0.

Pena, L. D., E. Calvo, I. Cacho, S. Eggins, and C. Pelejero (2005), Identification and removal of Mn-Mg-rich contaminant phases on foraminiferal tests: Implications for Mg/Ca past temperature reconstructions, *Geochem. Geophys. Geosyst.*, *6*, Q09P02, doi:10.1029/2005GC000930.

Pflaumann, U., et al. (2003), Glacial North Atlantic: Sea-surface conditions reconstructed by GLAMAP 2000, *Paleoceanography*, *18*(3), 1065, doi:10.1029/2002PA000774.

Pisias, N. G., P. U. Clark, and E. J. Brook (2010), Modes of global climate variability during Marine Isotope Stage 3(60–26 ka), *J. Clim.*, *23*(6), 1581–1588, doi:10.1175/2009JCLI3416.1.

Prahl, F. G., and S. G. Wakeham (1987), Calibration of unsaturation patterns in long-chain ketone compositions for palaeotemperature assessment, *Nature*, *330*(6146), 367–369, doi:10.1038/330367a0.

Rahmstorf, S. (2002), Ocean circulation and climate during the past 120,000 years, *Nature*, *419*(6903), 207–214, doi:10.1038/nature01090.

Rashid, H., and E. Grosjean (2006), Detecting the source of Heinrich layers: An organic geochemical study, *Paleoceanography*, *21*, PA3014, doi:10.1029/2005PA001240.

Rodrigues, T., A. H. L. Voelker, J. O. Grimalt, F. Abrantes, and F. Naughton (2011), Iberian Margin sea surface temperature during MIS 15 to 9(580–300 ka): Glacial suborbital variability vs interglacial stability, *Paleoceanography*, *26*, PA1204, doi:10.1029/2010PA001927.

Rosell-Melé, A., M. A. Maslin, J. R. Maxwell, and P. Schaeffer (1997), Biomarker evidence for "Heinrich" events, *Geochim. Cosmochim. Acta*, *61*(8), 1671–1678, doi:10.1016/S0016-7037(97)00046-X.

Rosell-Melé, A., E. Jansen, and M. Weinelt (2002), Appraisal of a molecular approach to infer variations in surface ocean freshwater inputs into the North Atlantic during the last glacial, *Global Planet. Change*, *34*(3–4), 143–152, doi:10.1016/S0921-8181(02)00111-X.

Roy, M., P. Clark, R. Barendregt, J. Glasmann, and R. Enkin (2004), Glacial stratigraphy and paleomagnetism of late Cenozoic deposits of the north-central United States, *Geol. Soc. Am. Bull.*, *116*, 30–41, doi:10.1130/B25325.1.

Ruddiman, W. F. (1977), Late Quaternary deposition of ice-rafted sand in the subpolar North Atlantic (lat 40° to 65°N), *Geol. Soc. Am. Bull.*, *88*(12), 1813–1827, doi:10.1130/0016-7606(1977)88<1813:LQDOIS>2.0.CO;2.

Ruddiman, W. F., M. E. Raymo, D. G. Martinson, B. M. Clement, and J. Backman (1989), Pleistocene evolution: Northern Hemisphere ice sheets and North Atlantic Ocean, *Paleoceanography*, *4*(4), 353–412, doi:10.1029/PA004i004p00353.

Schiebel, R., J. Bijma, and C. Hemleben (1997), Population dynamics of the planktic foraminifer Globigerina bulloides from the eastern North Atlantic, *Deep Sea Res., Part I*, *44*(9–10), 1701–1713, doi:10.1016/S0967-0637(97)00036-8.

Sigman, D., A. M. de Boer, and G. H. Haug (2007), Antarctic Stratification, atmospheric water vapor, and Heinrich Events: A hypothesis for Late Pleistocene deglaciations, in *Ocean Circulation: Mechanisms and Impacts, Geophys. Monogr. Ser.*, vol. 173, edited by A. Schmittner, J. Chiang, and S. Hemmings, pp. 335–349, AGU, Washington, D. C.

Stein, R., J. Hefter, J. Grützner, A. Voelker, and B. D. A. Naafs (2009), Variability of surface-water characteristics and Heinrich-like Events in the Pleistocene mid-latitude North Atlantic Ocean: Biomarker and XRD records from IODP Site U1313(MIS 16–9), *Paleoceanography*, *24*, PA2203, doi:10.1029/2008PA001639.

Swift, J. (1986), The Arctic waters, in *The Nordic Seas*, edited by B. G. Hurdle, pp. 129–151, Springer, New York.

Venz, K. A., D. A. Hodell, C. Stanton, and D. A. Warnke (1999), A 1.0 Myr record of glacial North Atlantic Intermediate Water variability from ODP Site 982 in the northeast Atlantic, *Paleoceanography*, *14*(1), 42–52, doi:10.1029/1998PA900013.

Voelker, A. H. L., T. Rodrigues, K. Billups, D. Oppo, J. McManus, R. Stein, J. Hefter, and J. O. Grimalt (2010), Variations in mid-latitude North Atlantic surface water properties during the mid-Brunhes (MIS 9–14) and their implications for the thermohaline circulation, *Clim. Past*, *6*, 531–552, doi:10.5194/cp-6-531-2010.

Weeks, A. R., M. J. R. Fasham, J. Aiken, D. S. Harbour, J. F. Read, and I. Bellan (1993), The spatial and temporal development of the spring bloom during the JGOFS North Atlantic Bloom Experiment, 1989, *J. Mar. Biol. Assoc. U. K.*, *73*(02), 253–282, doi:10.1017/S0025315400032847.

Wright, A. K., and B. P. Flower (2002), Surface and deep ocean circulation in the subpolar North Atlantic during the mid-Pleistocene revolution, *Paleoceanography*, *17*(4), 1068, doi:10.1029/2002PA000782.

P. Ferretti, Department of Environmental Sciences, Informatics and Statistics, University Ca' Foscari of Venice, Calle Larga Santa Marta 2137, Dorsoduro, I-30123 Venice, Italy.

G. H. Haug, Geological Institute, ETH Zürich, CH-8092 Zürich, Switzerland.

J. Hefter, B. D. A. Naafs, and R. Stein, Alfred Wegener Institute for Polar and Marine Research, Department of Marine Geology and Paleontology, Am Alten Hafen 26, D-27568 Bremerhaven, Germany. (david.naafs@awi.de)